000129 FILE

BOL	FIRST Bolometer	Doc No:RAL/N0006.3
	Title: Beam patterns in PHOT-BOL design & telescope Prepared by: Martin Caldwell	Date: 28/10/97

CIRCULATION:

Martin Caldwell	RAL
Peter Gray	RAL
Tony Richards	RAL
Bruce Swinyard	RAL
Roger Emery	RAL
Matt Griffin	QMW
Eli Atad	ROE
Walter Gear	ROE

CONTENTS.

0. Change summary.

All changes are marked by a line at the margin. This update is made for the following reasons (ref.4):

- Beam shape finalised to: gaussian beam from detector, clipped at 1/e^2 intensity by cold stop.
- To include estimated background levels due to portions of beam on optics surround (section 4)
-

3.1 Detector model & beam shape.

For beam propagation, the beam is first defined at the detector, and propagated outwards through the system. The detector response analysed is gaussian (ref.4):

For the geometric beam, the divergence is given by F, the geometric beam f-number at the detector, and for the gaussian model the beam waist radius wo is taken as

$$wo=2F\lambda/\pi$$

where λ is the longest wavelength (0.64mm). This gives a far-field beam whose pattern is clipped by the system aperture stop (that defining system F-number) at its $1/e^2$ intensity point.

The field-of-view extremes are taken as the centres of the end detectors of the array. Elsewhere an allowance for geometric aberrations is also included (ref.5), but this is not needed here as the aberrations are already present in the reverse ray-trace.

3.2 Spatial resolution and model accuracy.

The beam edge can be defined only to the limited spatial resolution of the numerical analysis. This resolution, or the 'sharpness' of the beam edge, is given roughly by the pixel size, which is limited by the size of the ray trace which can be made. In this note

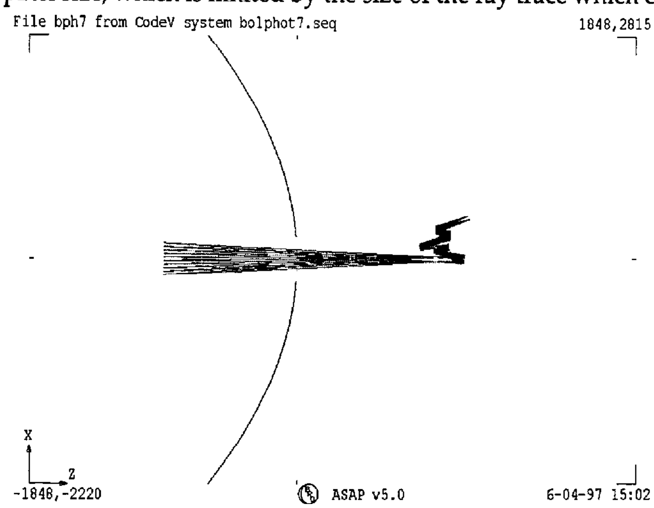

the beam is defined by a 30x30 pixel grid, so that 900 rays are traced per beam. Higher spatial resolution is not yet possible at the longer wavelengths, because the beam propagation algorithm requires that the spacing between rays is always much greater than the wavelength. This limitation may be overcome by using a more complicated ray-set (Gabor representation, ref.2), and this feature will be implemented in future work. In the results this limitation gives errors which increase during the reverse ray-trace and so are largest at the telescope mirrors (see figs 3 & 4, plots 1 & 2).

In the meantime, the diffraction actually modelled is that from a 'soft-edged' aperture, rather than the real 'hard-edged' aperture (a top-hat function energy transmission). As to the consequences of this, from the principles of Fourier optics we can say that the limited spatial resolution of the beam limits the angular range of the energy pattern in the far-field. Therefore the energy at larger diffraction angles is **underestimated** in the present analysis. The far-field angular range at which this effect is significant is estimated as roughly (λ/d) where d is the pupil ray spacing (spatial resolution). This implies that the patterns shown here are

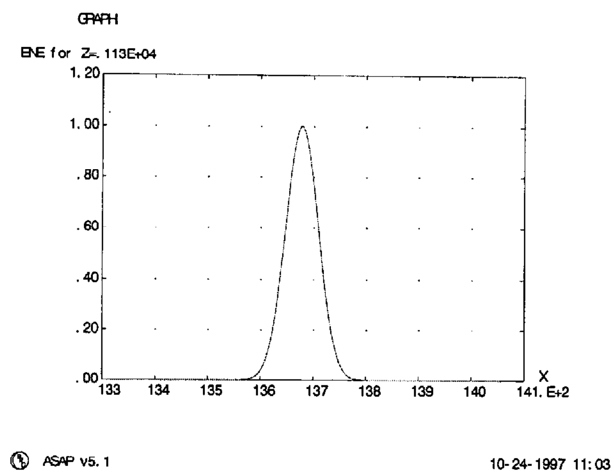

Fig.2 Beam pattern at detector plane λ=0.64mm. Horizontal axis is position in mm.

accurate up to about 30 x the Airy disc equivalent angular radius (λ/D where D is the pupil diameter).

3.3 Format of results.

The beam is propagated stepwise through the system, and is analysed at each component to give the beam profile. This is given in terms of optical intensity, i.e. flux per unit area. In this version all patterns show relative intensity only.

beams from each detector are co-incident, so that the clipping is the same at all positions in the field. Again, since the design is still changing, in this update we compute only the on-axis beam pattern & background level.

Using the format of the stray light analysis (ref.7), the background levels are expressed as a fraction of the level due to the primary & secondary mirrors (ε=0.01, T=80K), as this is near to the level of the ideal BLIP condition. This fraction is given by

$$\eta = \frac{\varepsilon_s . P(T_s) . \int BDDF(\Omega) . d\Omega}{2 . \varepsilon_t . P(T_t) .}$$

here Ω is the solid angle in the space in front of the component being considered and P(T) is the Planck black-body function. The calculation is for radiance in the longest wavelength band (worst-case, band 3 in ref.7). The subscripts s and t denote surround and telescope emissivities respectively. The factor 2 in the denomenator is to account for the two telescope mirrors.

The integral in the above equation is equivalent to the fraction of the beam flux which is on the surround surface, and this can be calculated from the beam patterns of section 6, taking into account that the patterns are actually 2-D. The table below shows the contributions so far calculated. Here the cold stop level is from the present data, the telescope obscuration level is as estimated from previous (top-hat beam) data of ref.6, and the M3 level is from the BDDF method of ref.7.

Component	**Surround emissivity**	**Temp.**	**Beam flux fraction**	**Fractional background, band 3**		**Assumptions**
				Centre detector	Outer detector	
Cold stop	1.0	2	0.006	0.007	0.007	Gaussian beam, narrow angle
M3 surround	0.15	80	-	0.21 Ref.7	-	BDDF analysis, top-hat beam, wide-angle: 7-15 deg.
rear-side of PM	0.15	80	0.0006	-	0.004 Ref.6.	Top-hat beam, narrow angle

Table. 1 Background levels due to beam clipping, given as fraction of telescope BLIP.

8. M3 (object 4)
9. Primary cut-out (object 3)
10. Telescope secondary (object 2)
11. Telescope primary (object 1)
12. Sky (object 12)

Figure 3. The following 12 plots show beam profiles at each component as listed above, for on-axis detector only.

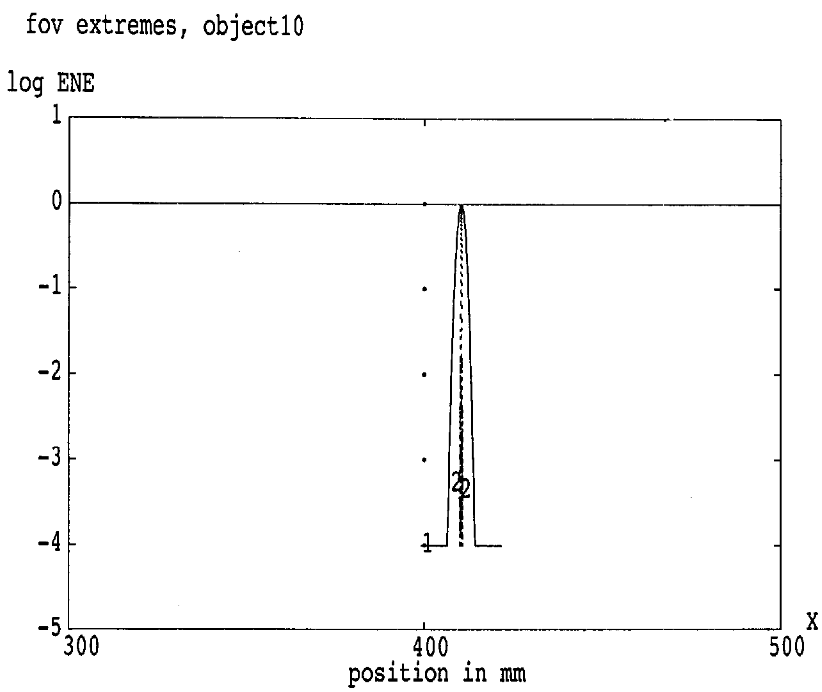

ASAP v5.1

10-23-1997 12:11

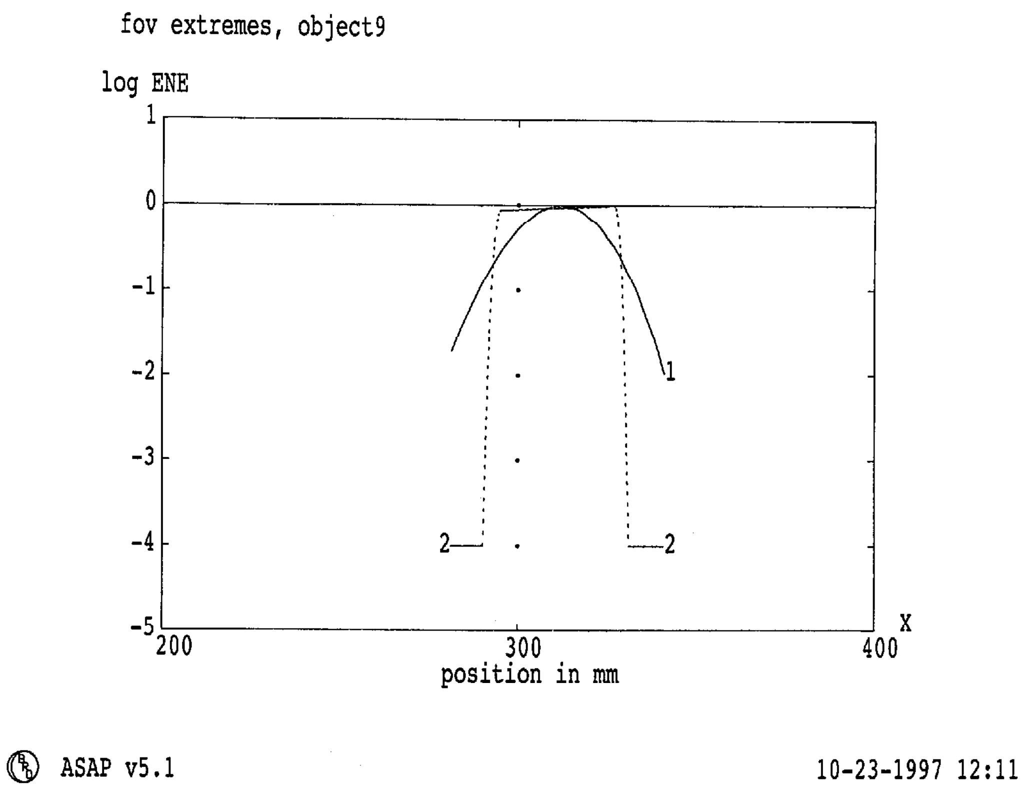
fov extremes, object9
log ENE
1
0
-1
-2
-3
-4
-5
1
2
2
X
200
300
400
position in mm
ASAP v5.1
10-23-1997 12:11

fov extremes, object8

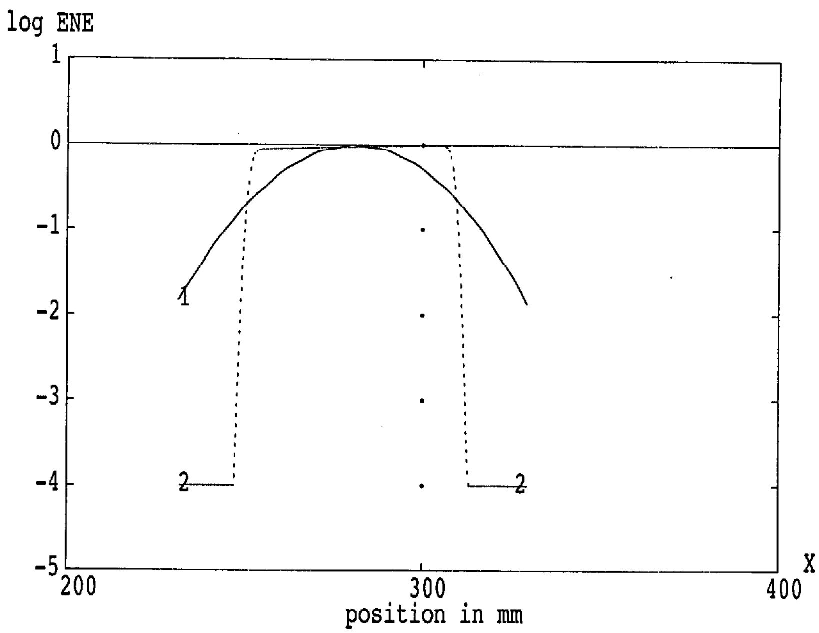

ASAP v5.1

10-23-1997 12:11

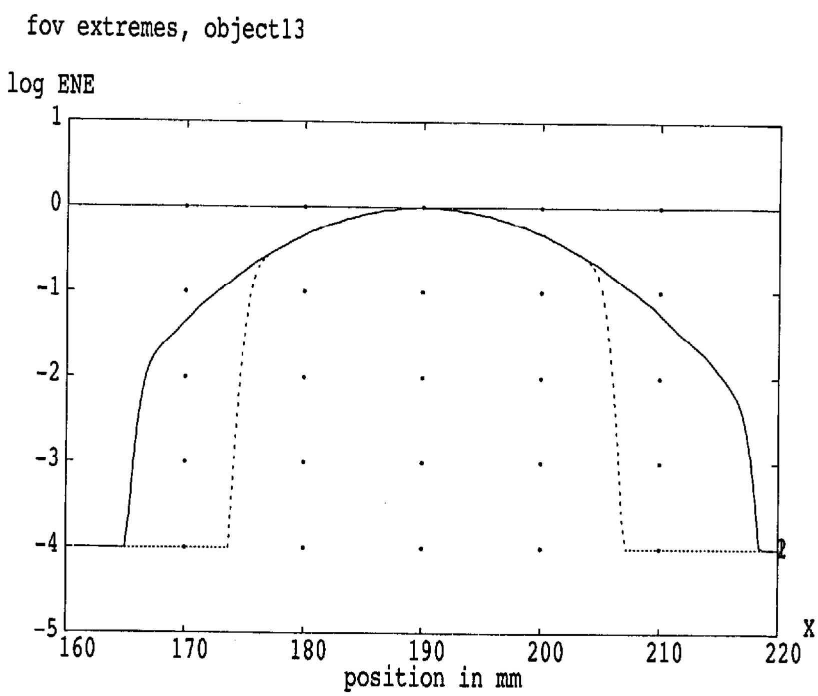

ASAP v5.1 10-23-1997 12:11

fov extremes, object7

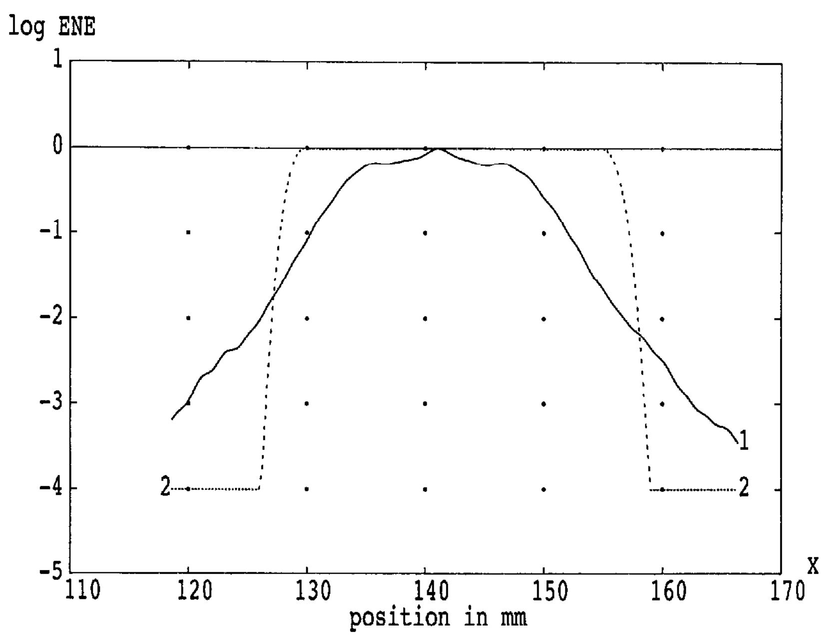

ASAP v5.1   10-23-1997 12:11

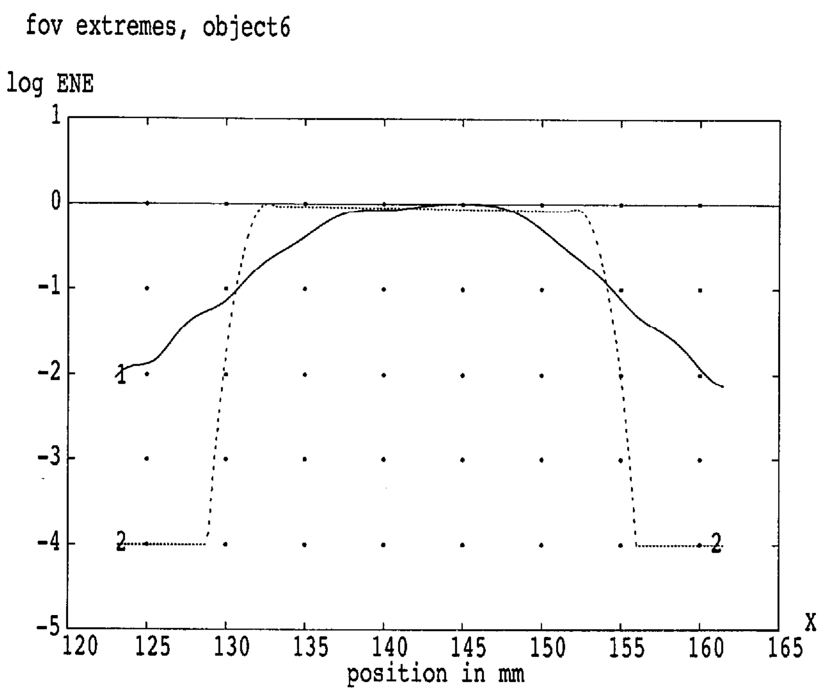

ASAP v5.1 10-23-1997 12:11

fov extremes, object5

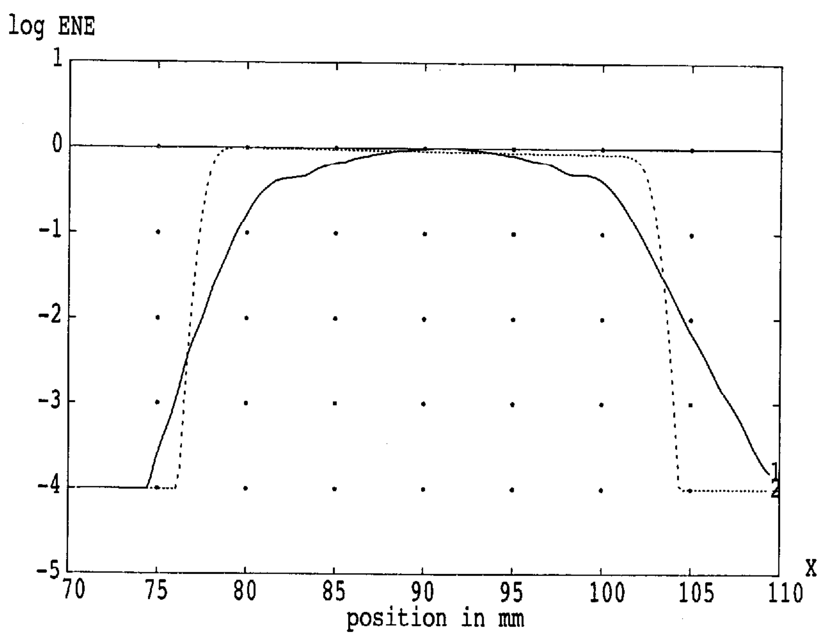

ASAP v5.1

10-23-1997 12:11

fov extremes, object4

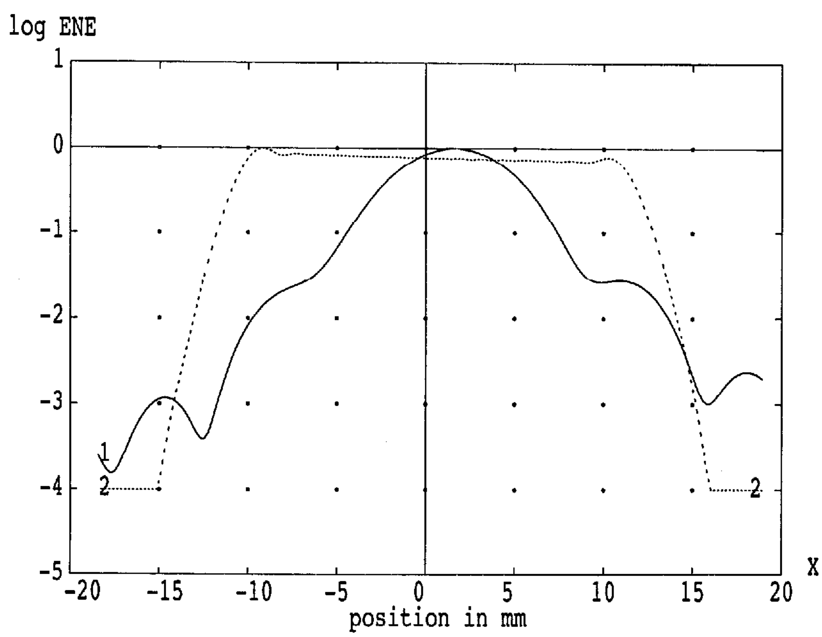

ASAP v5.1

10-23-1997 12:11

fov extremes, object3

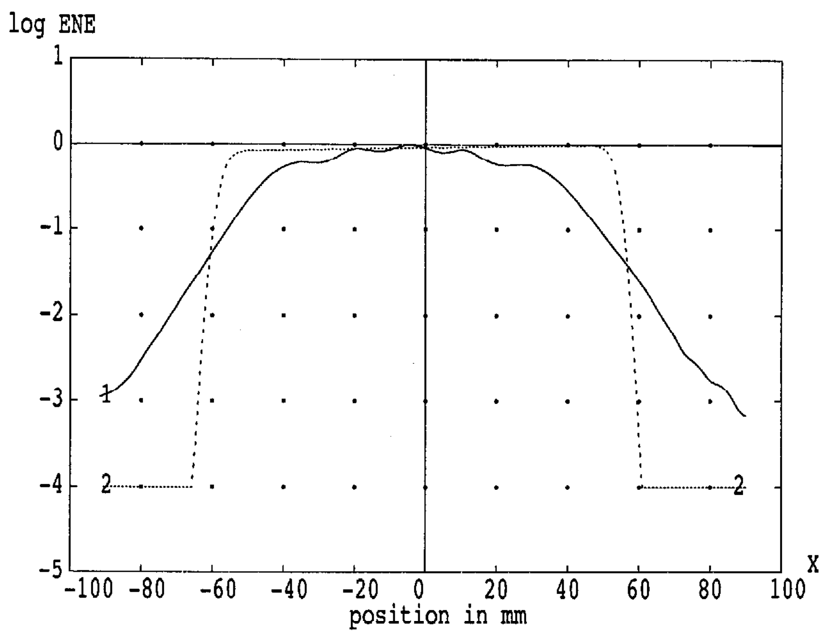

ASAP v5.1

10-23-1997 12:11

fov extremes, object2

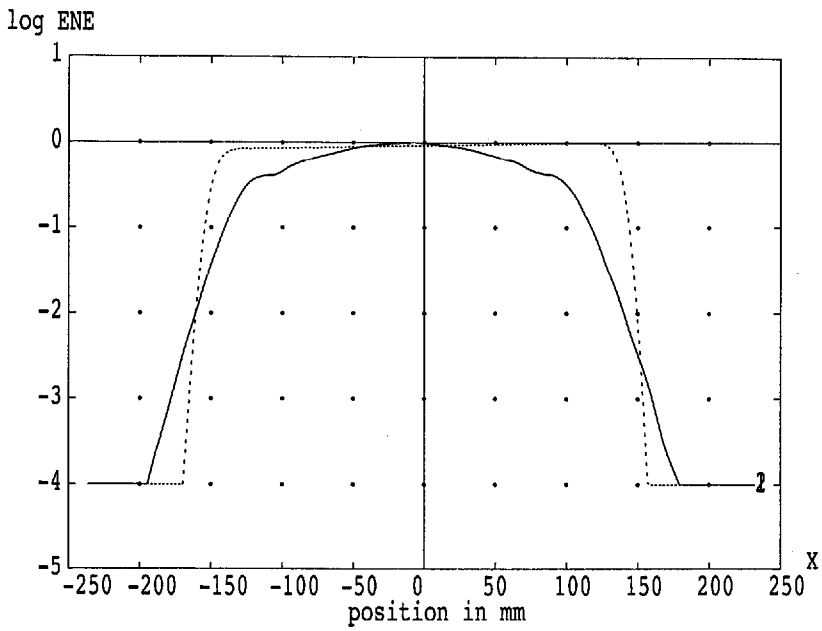

ASAP v5.1

10-23-1997 12:11

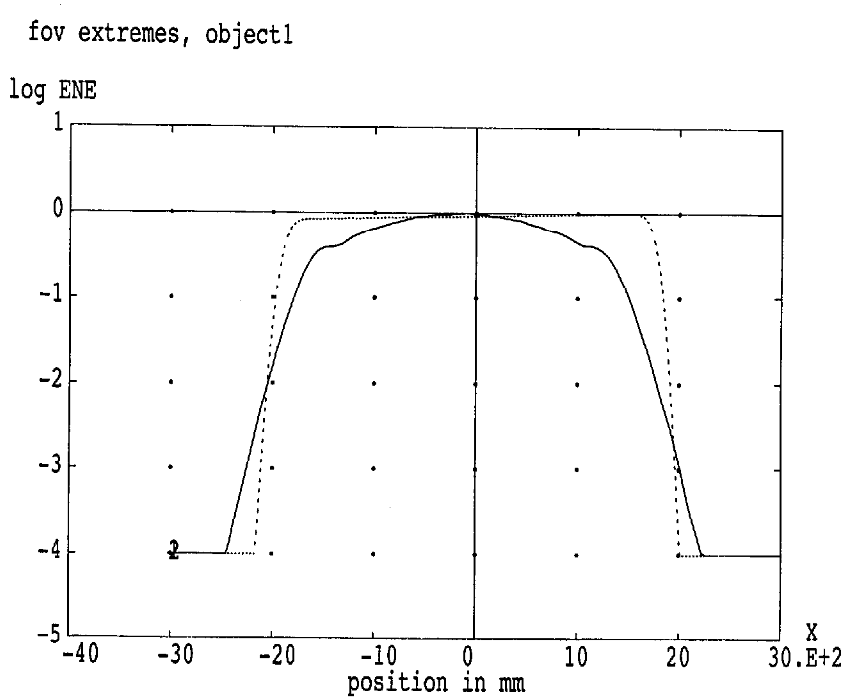

ASAP v5.1

10-23-1997 12:11

beam pattern, far-field

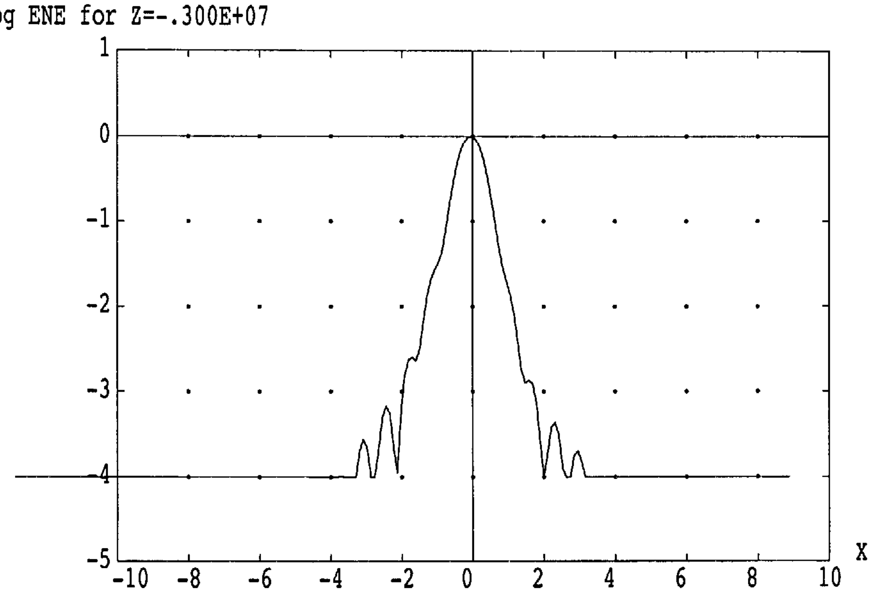

off-axis angle in arcmins

ASAP v5.1 10-23-1997 12:11